Journal of Chromatography A, 1218 (2011) 4234–4239

Contents lists available at ScienceDirect

Journal of Chromatography A

journal homepage: www.elsevier.com/locate/chroma

Separation and characterization of gold nanoparticle mixtures by flow-field-flow fractionation

Luigi Calzolai, Douglas Gilliland, César Pascual Garcìa, François Rossi*

European Commission, Joint Research Centre, Institute for Health and Consumer Protection, I-21027, Ispra (VA), Italy

ARTICLE INFO

Article history:
Available online 14 January 2011

Keywords:
Nanoparticles
Flow-field-flow fractionation
AF4
Dynamic light scattering
Nanotoxicity

ABSTRACT

We show that using asymmetric flow-field-flow fractionation and UV–vis detector it is possible to separate, characterize, and quantify the correct number size distribution of gold nanoparticle (AuNP) mixtures of various sizes in the 5–60 nm range for which simple dynamic light scattering measurements give misleading information. The size of the collected nanoparticles fractions can be determined both in solution and in the solid state, and their surface chemistry characterized by NMR. This method will find widespread applications both in the process of "size purification" after the synthesis of AuNP and in the identification and characterization of gold-based nanomaterials in consumer products.

1. Introduction

Nanotechnology is expected to have a large socio-economical impact in practically all industrial activity fields. The use of nanomaterials is constantly increasing in all industrial sectors, in particular in biomedicine with applications in diagnostics and therapeutics [1,2]. In particular gold nanoparticles have already several applications in biology and medicine [3]. For example the drug Aurimune™, that uses TNF protein bound to gold nanoparticles to target solid tumors, just completed Phase I clinical trials [4]. Gold nanoparticles are also used in consumer products such as cosmetics.

The effects of nanoscale objects on biological systems and their potential toxicity are currently the focus of widespread investigations. Recently the interaction of nanoparticles with proteins [5] has emerged as a key parameter in nanomedicine and nanotoxicology [6] and it is also quite clear that size, composition, and surface chemistry play an important role [7,8].

The fractionation and characterization of mixtures of nanoparticles is thus a key requirement for the assessment of their properties in toxicology testing or for their identification and size determination in consumer products. The proper size determination of different nanoparticles present in complex samples is a difficult problem. The standard approach to measure the size of nanoparticles in solution is to use dynamic light scattering (DLS) measurements. The technique can be applied to both diluted and concentrated solutions [9] but has a limited power at resolving mixtures mainly due to the fact that particles contribution to the scattering intensity depends by the sixth power of their radius [10,11]. The accurate and sensitive determination of size distribution of nanoparticles in complex mixtures will likely become even more important in the near future if the proposed definition of nanomaterial as containing more than 1% of the total number of particles in the 1–100 nm size range will be adopted by the European Union.

Flow-field-flow fractionation is a well established technique for the size-based separation of components of complex mixtures [12] in a wide range of fields from ultra-high molecular mass polymers [13], to nanoparticles in environmental conditions [14], and biomolecules [15]. Only a few studies have addressed the characterization of gold nanoparticles by AF4 [16–20]. In particular Rameshwar et al. [18] showed that in the case of a AuNP stabilized by mercaptosuccinic acid, using AF4 was possible to separate as-synthesized nanoparticles into fractions of different sizes. In their very recent paper Cho and Hackley [20] have showed how experimental conditions for the separation of gold nanoparticles can be optimized by controlling some parameters such as injection volume, mobile phase composition, membrane type and pore size.

In this work, using AF4 and high sensitive UV–Vis detection we developed a procedure for the efficient separation, size determination, chemical characterization, and quantification of the relative number of particles of different size starting from complex gold nanoparticle mixtures. The detailed analysis performed here is a fundamental requirement for the identification and correct quantification of the relative number size distribution of nanoparticles in consumer products and the toxicology testing of too often poorly characterized nanoparticles samples.

* Corresponding author. Tel.: +39 0332785443.
E-mail addresses: luigi.calzolai@jrc.ec.europa.eu (L. Calzolai), francois.rossi@jrc.ec.europa.eu (F. Rossi).

0021-9673/$ – see front matter © 2011 Elsevier B.V. All rights reserved.
doi:10.1016/j.chroma.2011.01.017

2. Materials and methods

2.1. Gold nanoparticles synthesis and sample preparation

2.1.1. 5 nm AuNP

Gold nanoparticles were produced by $NaBH_4$ (Sigma) reduction of a starting solution of sodium citrate (Sigma) (2.5 mM) and $HAuCl_4$ (Sigma) (0.5 mM) in water. Typically 100 mL of the starting solution was cooled in an ice bath to 4 °C before the reduction was initiated by the addition of 1 mL of freshly prepared ice-cold $NaBH_4$ solution (0.1 M) under rapid stirring. The formation of gold nanoparticles was observed to occur immediately as shown by the rapid colour change from pale yellow to wine red.

2.1.2. 15 nm AuNP

$HAuCl_4$ (0.5 mM) in water was rapidly heated to 97 °C in a microwave heating system (Discover S by CEM) and allowed to equilibrate for 5 min. The reaction was started by injection of sufficient sodium citrate (0.1 mM) to produce a final citrate concentration of 2.5 mM. The reaction mixture was then kept at 97 °C for 20 min after which the reaction vessel was rapidly cooled to room temperature.

2.1.3. 45 nm AuNP

100 mL of $HAuCl_4$ (0.5 mM) was heated to 97 °C in a microwave heating system and then allowed to stabilize for 5 min. The pH of this solution was then increased to >10 by the addition of 1.1 mL of NaOH (0.2 M). At this point the reduction reaction was started by injecting sodium citrate (0.01 mM) solution to produce a final citrate concentration of 0.5 mM. The higher pH of this mixture ensured that the reduction of gold by citrate proceeds slowly with the formation of a smaller number of larger particles. The solution was maintained at 97 °C for 20 min at which point the solution was seen to be a slightly purple/pink color indicating the partial conversion of the gold salt into gold nanoparticles. The solution was then cooled to 90 °C under stirring at which point 1 mL of NaOH (0.2 M) then 2.5 mL of $NH_2OH{\cdot}HCl$ (0.1 M) were injected into the solution. The addition of $NH_2OH{\cdot}HCl$ promotes the reduction of the remaining gold ions in solution selectively on the surface of existing gold nanoparticles, thus increasing the size of the existing particles rather than nucleating new particles. The second addition of NaOH serves to adjust the pH of the final solution to value of around 6.5–6.8 which is comparable with the other two synthesis methods.

2.2. Asymmetric flow-field flow fractionation

Fractionation of AuNP mixture was carried out using a AF4 system (AF2000 *Postnova Analytics*, Germany). The channel used was 29 cm long with a spacer of 350 μm and a regenerated cellulose membrane with a 10 kDa cutoff. The flows were provided by two separate pumps and the cross-flow was realized by a separate piston pump which is continuously adjustable. The eluent was ultrapure MilliQ water and was degassed by sonication with a water bath sonicator and with a vacuum degasser just before delivery and the flow kept at 0.5 mL/min. Optimal separation of the three components was achieved using a constant cross-flow of degassed MilliQ water of 2 mL/min for the first 10′, a linear gradient 2–0 mL for the next 10′, and then 0 mL/min for the last 10′. The output from the channel was connected to an on-line UV–Vis spectrometer set at 525 nm wavelength for detection of AuNP. The injection volume was 20 μL and each fraction of 500 μL was collected with an automatic fraction collector.

2.3. Particle size distribution

Particle size distribution (PSD) was determined by dynamic light scattering (DLS) using a Malvern Zetasizer Nano-ZS instrument with temperature control. Each sample was recorded at 25 ± 1 °C, in triplicate; each measurement is the average of 20 data sets acquired for 10 s each. Hydrodynamic diameters have been calculated using the internal software analysis from the DLS intensity-weighted particle size distribution.

2.4. Scanning electron microscopy

Samples were studied with a scanning electron microscope (SEM) FEI Nova 600I Nanolab, using relatively low acceleration voltages (5 kV) that allow immersion lens detection without significant loss of resolution. Samples were prepared by spotting 2 μL of solution on clean conductive silicon (n-doped) to avoid charging effects on the images. The drying was performed on a warm hotplate. Images were taken before and after 30 min of UV/ozone treatment used to clean some possible organic matrix around the nanoparticles. The image of the samples treated with UV radiation exhibited some improvement that could be better appreciated for smallest size nanoparticles.

2.5. UV–vis spectra

UV–vis spectra were recorded at room temperature with a Thermo Nicolet Evolution 300 instrument in the 190–800 nm range using 1-cm path length quartz cuvettes and 1.5 nm bandwidth. Recorded spectra were smoothed with a 20 point smoothing average function.

2.6. NMR spectroscopy

Samples for NMR experiments were prepared by transferring 450 μL of sample from selected fractions into NMR tubes and addition of 20 μL D_2O. ^1H NMR experiments were collected with a 500 MHz Bruker instrument using an excitation sculpting pulse sequence for water suppression [21] and 256 scans. Data were processed with the same processing parameters for all samples using the TopSpin NMR software.

3. Results

We synthesized well defined gold nanoparticles (citrate stabilized) of three different sizes below 100 nm. The three different AuNP preparations (termed 5 nm AuNP, 15 nm AuNP, and 45 nm AuNP) were well mono-dispersed with mean hydrodynamic diameters (D_h) of 6.1, 17.4, and 43.7 nm (as obtained by DLS) and polydispersivity indexes (PdI) of 0.15, 0.09, and 0.12, respectively (see Fig. 1A).

To study the behavior of complex AuNP mixtures and to develop methods for their separation based on size, we prepared a sample containing an equal volume amount of these three AuNP samples. The various AuNP samples were synthesized starting from the same amount of $HAuCl_4$, thus equal volumes contain many more small AuNP compared to larger. Based on the dimensions of the three different AuNP preparations the relative number of particles in the mixture can be estimated to be around 350:15:1 for the 6.1, 17.4, and 43.7 nm AuNP, respectively.

Fig. 1B shows the particle size distribution of this gold mixture in water (1:1:1 volume mixture of 5 nm AuNP, 15 nm AuNP, and 45 nm AuNP); it has a mean hydrodynamic diameter of 41.9 nm and a polydispersivity index of 0.21. So basically the DLS measurement indicates the presence of particles with a hydrodynamic

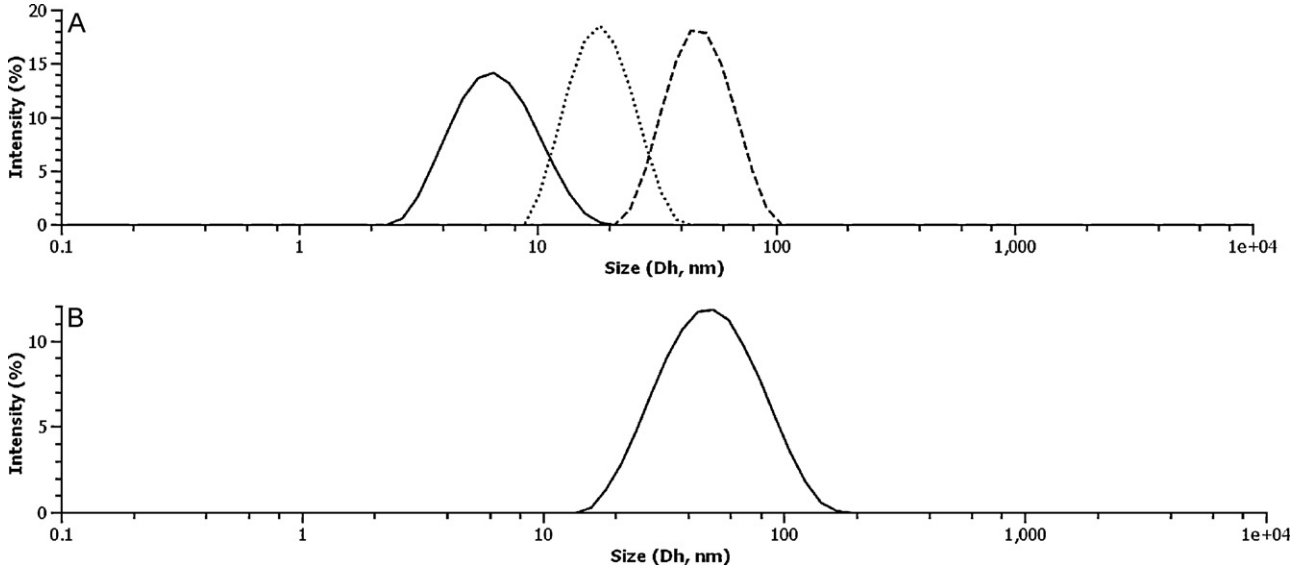

Fig. 1. Particle size distribution of gold nanoparticles obtained by DLS measurements. (A) PSD of individual AuNP preparations (5 nm AuNP continuous line, 15 nm AuNP dotted line, and 45 nm AuNP dashed line). (B) PSD distribution of 1:1:1 mixture of 5 nm AuNP, 15 nm AuNP, and 45 nm AuNP.

diameter slightly smaller than the biggest particles in the mixture and an increased polydispersivity index. These results could be caused by two effects: a well known difficulty of DLS measurements in resolving particles which have less than a factor of 3 size difference [11] or a real aggregation of some smaller nanoparticles towards bigger ones in the mixture. The two effects are not mutually exclusive and both of them could contribute to the shift towards larger hydrodynamic diameter and increased polidispersivity for the AuNP mixture.

The scanning electron microscopy images of the AuNP mixture shown in Fig. 2A indicate that the sample still contains particles of at least three different sizes of around 5, 20, and 50 nm and a few quite larger aggregates.

To separate the AuNP mixture into the individual components we used asymmetric flow-field-flow fractionation. The cross-flow field in AF4 leads to an accumulation of the analyte species at the bottom of the channel. When the effects opposing the cross-flow force are dominated by diffusion the system is operating in the so-called normal-mode FFF or diffusion-mode FFF and the analyte components with small hydrodynamic diameter will elute from the channel before large particles. In the case of larger particles the system is operating in the steric-mode FFF (usually above 1 μm) [22]. In this situation diffusion is negligible in opposing the primary driving force of the cross-flow and the large particles reach a state of equilibrium in close proximity to the wall. The end result is that large particles are displaced more rapidly by flow and are eluted earlier than the small particles.

Fig. 3A shows the fractogram obtained after injection of 20 μL of AuNP mixture using a constant cross-flow of 2 mL/min for the first 10′, a linear gradient 2–0 mL for the next 10′, and then 0 mL/min for the last 10′. The different fractions have been collected at time intervals of 1′ each, allowing the off-line characterization of the various fractions. The UV–vis detector has been set to 525 nm, at a wavelength specific for the plasmon resonance band of gold nanoparticles (see Fig. 4). The fractogram in Fig. 3A shows the presence of three well distinct peaks of AuNP with retention times of around 10′, 14′, and 20′.

The cross-flow rate was optimized by performing test runs at constant cross-flow rates of 1, 2, and 3 mL/min. The most promising condition (2 mL/min) was then optimized by adding a linear gradient (2–0 mL/min) after the appearance of the first peak containing the small particles at time 10′.

Fig. 3B shows the hydrodynamic radius (measured by DLS) of selected fractions and the trend in sizes is consistent with the above picture with smaller particles exiting first and a general increase in particle size with time. The mean counts per second (CPS) values from the DLS measurements of the fractions are shown in Fig. 3C. Early fractions have very low CPS values, with a slight increase in correspondence of Peak 1 at 11′, Peak 2 at 14′, and a clear maximum for Peak 3 at 20′.

The hydrodynamic diameter of fractions around Peak 1 could not be measured due to low concentration of the sample and the fact that in the Rayleigh approximation the intensity of scattered light depends by r^{-6} of the particle radius (r) and thus smaller particles scatter light much less efficiently. Peak 2 has an average D_h of 26 nm and Peak 3 average D_h of 54 nm, both with polydispersivity indexes below 0.2. Fraction 26 has an average size of 82 nm with a PdI of 0.39 indicating that it is not monodispersed and a high resolution analysis of the DLS data indicates the presence of aggregates larger than 2 μm.

The above data indicate that the separation was operating (as expected due to the relatively small size of the particles) in the normal-mode FFF with small particles exiting the channel before larger ones.

The SEM images of Peaks 1–3 in Fig. 2 show that AF4 fractionation has been able to separate the AuNP mixture into fractions of homogenous sizes of around 8 nm, 20 nm, and 45 nm. In particular the fractionation process has been able to remove large size aggregates that are for example present in the original mixture (Fig. 2A) and large particles are not present in Peak 1 that contains only very small particles (Fig. 2B).

The integrals of the three peaks present in the fractogram of the AF4 separation (obtained by detecting the absorbance at 525 nm) of the AuNP mixture are proportional to the amount of nanoparticles present in each peak: it is thus possible to estimate the relative number of particles present in the different peaks from the measurement of these integrals. A complication arises due to the fact that the extinction coefficient of the surface resonance band of AuNP responsible for the absorbance at 525 nm strongly depends by the particle size. The molar extinction coefficient, ε, of AuNP of different sizes can be calculated by the equation [23]:

$$\ln \varepsilon = k \ln D + a$$

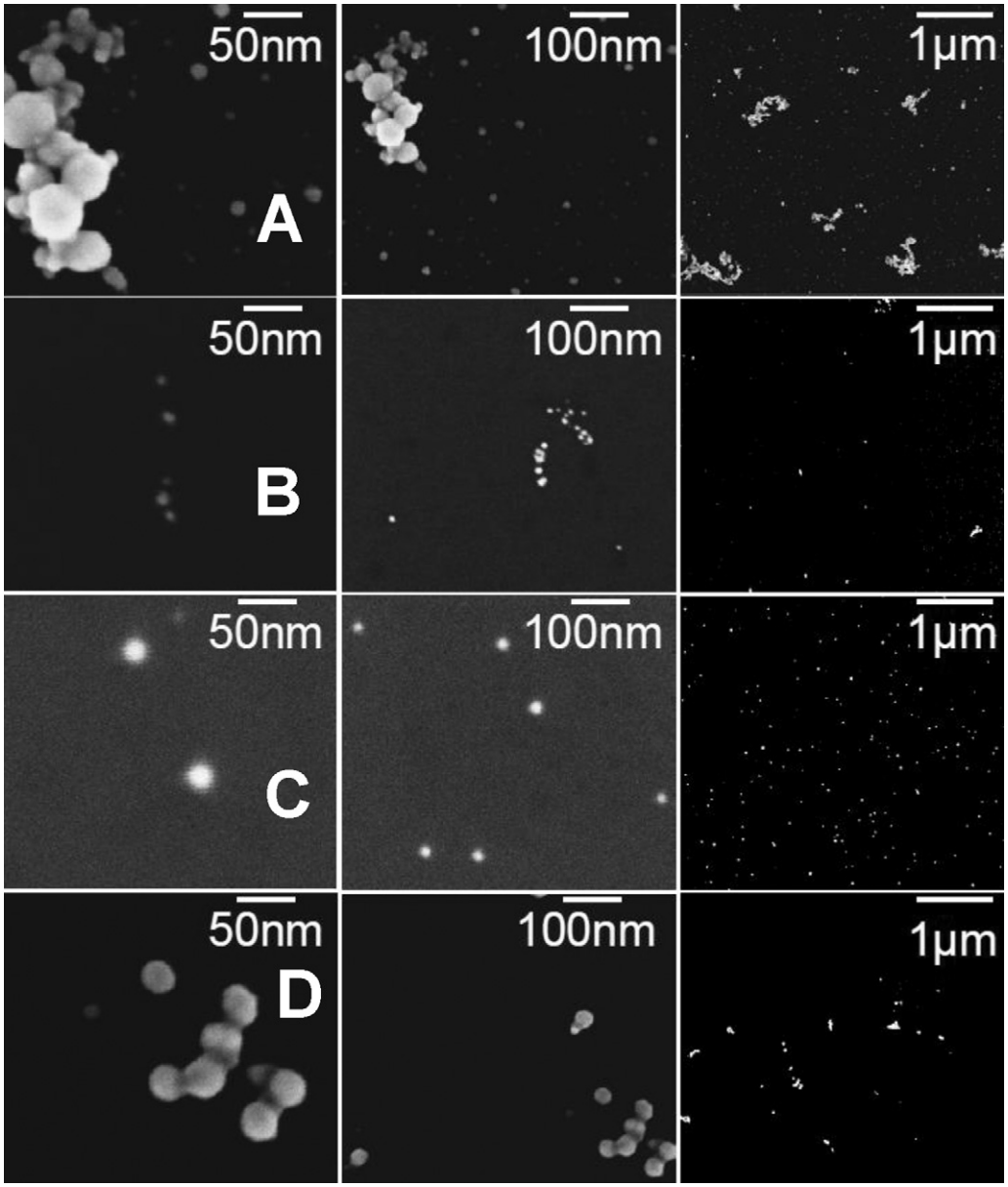

Fig. 2. Scanning electron micrograph of gold nanoparticles. (A) Mixture of 1:1:1 of 5 nm AuNP, 15 nm AuNP, and 45 nm AuNP. (B) Peak 1 of AF4 fractogram. (C) Peak 2 of AF4 fractogram. (D) Peak 3 of AF4 fractogram.

where D is the diameter of the nanoparticles in nm, $k = 3.32$, $a = 10.80$.

From this equation we have calculated the molar extinction coefficient for the three different AuNP sizes (using the diameter obtained from the number particle size distribution of DLS data) as 1×10^7, 6.5×10^8, and 1.3×10^{10}, for the small, medium, and large AuNP, respectively. The number of nanoparticles for each component of the AuNP mixture is proportional to the integral of its peak in the fractogram divided by the molar extinction coefficient. Thus,

$$(\text{No. of particles})_i = \frac{I_i}{\varepsilon_i}$$

with integral values of 12, 34, and 54, for the small, medium, and large AuNP, respectively. The relative number of particles for the three peaks can thus be estimated by taking the ratios:

$$\frac{I_i/\varepsilon_i}{I_j/\varepsilon_j}$$

In this way we can estimate the relative number of particles present in the three AF4 peaks to be 290:12.7:1. These relative ratios are in quite good agreement with the number of particle ratios of 350:15:1 for the small, medium, and large AuNP samples, which have been used to prepare the AuNP mixture.

To better characterize the different fractogram peaks we recorded the ^{1}H NMR spectra of the original mixture and of Peaks 1–3. The NMR spectra in Fig. 5 show that the original mixture contains an excess of citrate used to stabilize the gold nanoparticles, while free citrate is not present in the NMR spectra of AF4 peaks. Comparing the NMR spectra of the original mixture and of the AF4 peaks it is possible to estimate that the eventual residual concentration of free citrate in the AF4 peaks to be below 100 nM. While it is possible to identify the presence or absence of free citrate in the various AuNP samples, it is not possible at the moment to reach any conclusion on the citrate molecules bound to AuNP because the chemical shift of such species has not yet been identified.

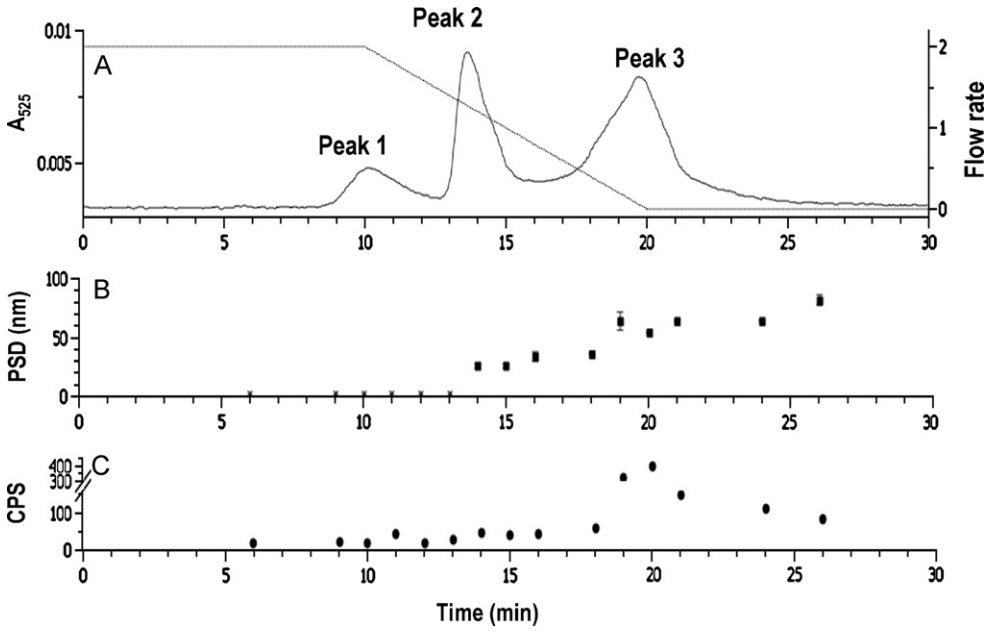

Fig. 3. Separation of gold nanoparticle mixture of 1:1:1 of 5 nm AuNP, 15 nm AuNP, and 45 nm AuNP by AF4. (A) Fractogram of AuNP mixture detected by on-line UV–vis measurement at 525 nm (continuous line, left *y*-scale), the cross-flow program used for the separation is shown (dotted line, right *y*-scale). (B) Mean diameter of particle size distribution of collected fractions. Fractions for which the DLS intensity is too low to allow a measurement are indicated by *. (C) Average Count per Seconds (CPS) of DLS measurements for some collected fractions.

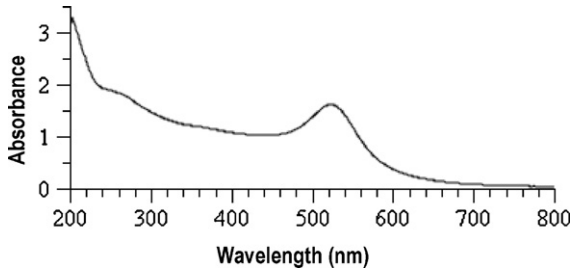

Fig. 4. UV–vis spectrum of the original AuNP mixture of 1:1:1 of 5 nm AuNP, 15 nm AuNP, and 45 nm AuNP.

4. Discussion

The determination of the size of nanoparticles in complex mixtures is a challenging problem, but the correct identification of the size and surface chemistry of nanoparticles is a key parameter for the proper assessment of the relationship between properties and toxicity of nanoparticles. For example in *in vitro* tests NP smaller than 5–10 nm can easily enter cells and it has been proven that AuNP toxicity strongly depends on the size of the nanoparticles [7]. Our results show that in the case of mixtures of nanoparticles of different sizes the direct measurement in solution of the particle size distribution does not correctly represent the sample (see Fig. 1). If we had used this mixture for toxicity testing we would have treated it as a mildly polydispersed AuNP sample of around 40 nm, when in reality it contains a combination of 5, 20, and 45 nm AuNP, with small particles representing the majority in terms of particle numbers. The situation is intrinsic in the use of DLS measurements and relates to the inability of the technique in resolving particles with sizes that are less than 3–4 times of each other [10,24] and to the fact that the intensity of the scattered light is inversely proportional to sixth power of the radius of the nanoparticle. Thus a 50 nm particle will scatter 10^6 as much light as a 5 nm particle. Direct SEM images of the mixture sample are useful, but they are also somehow constrained by the fact that they relate to samples in the dry state and thus the behavior of the same sample in solution could be different. For example the removal of solvent could artificially increase the aggregation of the particles.

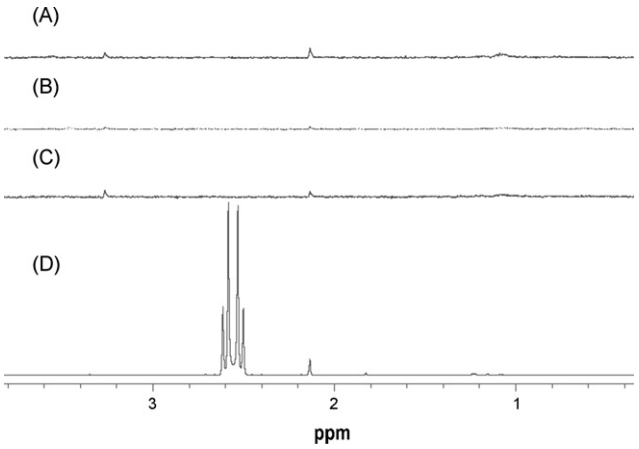

Fig. 5. ^{1}H NMR spectra of peaks of AF4 fractogram of AuNP mixture: Peak 1 (A), Peak 2 (B), Peak 3 (C), and starting AuNP mixture (D). The spectrum of AuNP mixture has been scaled down 8 times compared to spectra A–C.

All these considerations highlight the importance of verifying the "real" size of particles present in the sample by a method that separates particles based on their size. In this respect, asymmetric field flow fractionation has given very good results in separating a quite challenging AuNP mixture of nanoparticles in the 5–60 nm range. It has been possible to separate the mixture injecting a very low volume of 20 μL and the AuNP peaks in the fractogram have been detected using a simple UV–Vis detector tuned at the plasmon resonance frequency specific of gold nanoparticle. Using the integral of the peaks from the fractogram and the calculated extinction coefficient for the AuNP of different size it has been possible to estimate with good accuracy the relative number of particles of the three different sizes. These results represent a clear-cut example of the effectiveness of AF4 in detecting the real

number size distribution of mixtures of nanoparticles of different sizes.

The possibility of collecting the different fractions allows the extensive off-line characterization of the different AuNP peaks using non-destructive techniques such as NMR, DLS, and UV–Vis. NMR indicates that while the original mixture contains an excess of citrate that is used as stabilizer for the bare AuNP, the citrate is not present in the AF4-separated peaks.

Recently sedimentation field flow fractionation (SdFFF), which uses the centrifugal force [25] as the perpendicular field, has been used to study the synthesis of gold nanoparticles with good results [26]. In that example the use of SdFFF was limited to the analysis of the size distribution of different methods for the synthesis of gold nanoparticle and no attempt was made to separate complex mixtures of nanoparticles. In general SdFFF involves instrumentation that is more technically complex than AF4 [15]. In addition AF4 has the advantage of using relatively low cost semi-permeable membranes in the separation channel.

The use of AF4 for the separation and characterization of complex mixtures of nanoparticles will be particularly useful in two scenarios: for the preparation of NP samples with narrow particle size distributions and the identification of nanomaterials in consumer products. It is easy to envision situations where AF4 will be used for the "size purification" of nanoparticles preparations: instead of the time consuming and expensive process of optimization of the synthetic procedure a rough synthesis could be followed by a "size-purification" step by AF4. This approach could also take advantage of the availability of semi-preparative separation channels. The other scenario is made all the more urgent by the continuous increase in the use of nanoparticles in several consumer products and by the introduction of the labeling requirements for the presence of nanomaterials in cosmetic recently introduced in the European Union legislation. While the identification of the bulk material is quite straightforward with current technologies the determination of the number size distribution, especially below 100 nm, will be challenging and the current results are very encouraging on the capabilities of AF4 to solve these problems.

Acknowledgment

We would like to thank Dr. Thorsten Klein of Postnova analytics for useful discussion on the use of AF4 separation.

References

[1] J. Panyam, V. Labhasetwar, Adv. Drug Deliv. Rev. 55 (2003) 329.
[2] X. Michalet, F.F. Pinaud, L.A. Bentolila, J.M. Tsay, S. Doose, J.J. Li, G. Sundaresan, A.M. Wu, S.S. Gambhir, S. Weiss, Science 307 (2005) 538.
[3] X. Huang, P.K. Jain, I.H. El-Sayed, M.A. El-Sayed, Nanomedicine (Lond.) 2 (2007) 681.
[4] R. Goel, N. Shah, R. Visaria, G.F. Paciotti, J.C. Bischof, Nanomedicine (Lond.) 4 (2009) 401.
[5] L. Calzolai, F. Franchini, D. Gilliland, F. Rossi, Nano Lett. 10 (2010) 3101.
[6] M. Lundqvist, J. Stigler, G. Elia, I. Lynch, T. Cedervall, K.A. Dawson, Proc. Natl. Acad. Sci. U. S. A. 105 (2008) 14265.
[7] Y. Pan, S. Neuss, A. Leifert, M. Fischler, F. Wen, U. Simon, G. Schmid, W. Brandau, W. Jahnen-Dechent, Small 3 (2007) 1941.
[8] H.J. Yen, S.H. Hsu, C.L. Tsai, Small 5 (2009) 1553.
[9] M. Kaszuba, M.T. Connah, F.K. McNeil-Watson, U. Nobbmann, Partic. Partic. Syst. Charact. 24 (2007) 159.
[10] B.J. Berne, R. Pecora, Dynamic Light Scattering: With Applications to Chemistry, Biology, and Physics, Dover Publications, Mineola, NY, 2000.
[11] V.M. Gun'ko, A.V. Klyueva, Y.N. Levchuk, R. Leboda, Adv. Colloid Interface Sci. 105 (2003) 201.
[12] J.C. Giddings, Science 260 (1993) 1456.
[13] T. Otte, R. Brull, T. Macko, H. Pasch, T. Klein, J. Chromatogr. A 1217 (2010) 722.
[14] S.A. Cumberland, J.R. Lead, J. Chromatogr. A 1216 (2009) 9099.
[15] B. Roda, A. Zattoni, P. Reschiglian, M.H. Moon, M. Mirasoli, E. Michelini, A. Roda, Anal. Chim. Acta 635 (2009) 132.
[16] A. Zattoni, D.C. Rambaldi, P. Reschiglian, M. Melucci, S. Krol, A.M. Garcia, A. Sanz-Medel, D. Roessner, C. Johann, J. Chromatogr. A 1216 (2009) 9106.
[17] J.H. Song, W.-S. Kim, D.W. Lee, J. Liq. Chromatogr. Relat. Technol. 26 (2003) 3003.
[18] T. Rameshwar, S. Samal, S. Lee, S. Kim, J. Cho, I.S. Kim, J. Nanosci. Nanotechnol. 6 (2006) 2461.
[19] W. Sermsri, P. Jarujamrus, J. Shiowatana, A. Siripinyanond, Anal. Bioanal. Chem. 396 (2010) 3079.
[20] T.J. Cho, V.A. Hackley, Anal. Bioanal. Chem. 398 (2003).
[21] T.L. Hwang, A.J. Shaka, J. Magn. Reson. Ser. A 112 (1995) 275.
[22] S.K. Ratanathanawongs, J.C. Giddings, Anal. Chem. 64 (1992) 6.
[23] X. Liu, M. Atwater, J. Wang, Q. Huo, Colloids Surf. B Biointerfaces 58 (2007) 3.
[24] M. Kaszuba, D. McKnight, M. Connah, F. McNeil-Watson, U. Nobbmann, J. Nanopartic. Res. 10 (2008) 823.
[25] M.E. Schimpf, K. Caldwell, J.C. Giddings, Field Flow Fractionation Handbook, Wiley–Interscience, New York, 2000.
[26] C. Contado, R. Argazzi, J. Chromatogr. A 1216 (2009) 9088.